High power switching with a *V/n* oil switch

N. R. Pereira[a] and N. A. Gondarenko[b]
Berkeley Research Associates, P.O. Box 852, Springfield, Virginia 22150

(Received 2 May 1995; accepted for publication 22 September 1995)

Accurate switching is necessary to get reproducible pulses with minimal jitter from pulse power equipment. On a 10 MV pulse power machine, Aurora, we have improved the triggering of the oil closing switch in various ways. These include suppressing fast current oscillations during capacitive charging of the switch electrodes, using a faster trigger pulse that acts only during a fraction of the switch closure time, and localization of the arc. With additional use of the machine's symmetry the output pulses are now reproducible to better than 2% over the entire pulse shape, and the jitter is reduced about twofold, to 5 ns. © *1996 American Institute of Physics.* [S0021-8979(96)08301-8]

I. INTRODUCTION

This article studies the triggered breakdown of a large V/n oil switch.[1,2] The oil switch is the crucial element that determines the shape and timing of the pulse on Aurora,[3] a nominal 14 TW electron accelerator. One of these switches is needed for each of Aurora's four parallel Blumleins. Each Blumlein[4] consists of a 7 m (23 ft) diam outer shell with two nested cylinders inside. The middle one is charged on a microsecond time scale, and discharged on a 100 ns time scale through the switch under study here. A Blumlein pulse forming line gives the output pulse on a matched transmission line the same amplitude as the charging voltage. For Aurora the maximum voltage is about 12 MV, and the operational voltage is about 8 MV.

Aurora's oil switch is a V/n field distortion switch, a switch wherein the trigger electrode is charged to a constant fraction (''n'') of the switch voltage (''V''). On Aurora $n \simeq 10$, for a trigger voltage of about 0.8 MV. The switch is triggered by rapidly ($\sim$10 ns) discharging the trigger electrode through a smaller switch, here a conventional trigatron[5] gas switch. An oil arc forms, which closes the switch.

This work is part of an ongoing effort to reduce Aurora's jitter.[6–8] Other attempts to lower jitter tried to increase the trigger's voltage rate of rise,[9] but the results were ambiguous.

Here the approach is to identify the parameters that might affect switch closure time, and to control these parameters as best we can. Controllable parameters are the voltage across the switch, and the voltage wave form on the trigger electrode during charging and triggering. More difficult to control is the current through the oil arc. The current contact can be fixed by initiating a single arc, but control of the arc itself has so far proved elusive.

For gas switches, faster triggering and closure with a predefined arc are well-known ways to improve jitter. In Aurora's original oil switch a fast trigger pulse was deliberately avoided because it was thought that the trigger voltage should remain high while the switch is closing. However, once the arc is formed the trigger voltage turns out to be irrelevant. Likewise, the original switch wanted to trigger many parallel arcs to minimize the switch inductance. However, in practice the switch closes with at most three parallel arcs, and in positive polarity with only a single arc.[10] A single arc is unacceptable for low-impedance machines, but for Aurora's relatively high impedance $Z \simeq 20\Omega$, a single arc gives a sufficiently low inductance ($L \simeq 300$ nH) for an acceptable output rise time of $r = L/Z \simeq 30$ ns. A bonus of a single arc is that it produces a virtually identical pulse shape on different shots, provided the arc is always in the same position.[11]

Besides technological interest in reducing jitter, studies of triggered oil breakdown on a machine with Aurora's size accesses a parameter regime for electric breakdown of liquids that is unavailable elsewhere.[12] Aurora's arcs are 0.5 m long, and carry currents on the order of 100 kA at 10 MV. Related work[13] is in a complementary parameter regime with a much smaller scale, where many identical shots enable fundamental work (such as Ref. 14 for nonpolar liquids, Ref. 15 for water, and Ref. 16 or 17 for perspectives).

Here the motivation is technological (similar to Ref. 18).

II. ELECTRICAL MEASUREMENTS

Figure 1 shows the geometry of the oil switch region. The oil switch is the shaded region between a flat plate connected to the intermediate Blumlein electrode, and the hole surrounded by a torus in the inner electrode. The intermediate Blumlein carries the high voltage, while the voltage on the inner Blumlein electrode is close to ground (i.e., the outer electrode that is also the outer shell of the machine). The high voltage electrode of the switch is a flat plate about 55 cm away from the torus. Oil gives the entire volume a dielectric constant $\epsilon_r = 2.3$. The gas switch, which triggers the oil switch, is the structure on the cantilevered pipe in the center. It consists of a hot electrode to the left, connected to the oil switch trigger electrode, and a ground electrode to the right. The gas switch is triggered from outside the machine through a cable (not shown).

Voltage diagnostics in this region are capacitive monitors, shown at the numbered arrows. Probe 1 on the inner electrode looks at $\dot{V}_s$, the voltage on the oil switch hot electrode, while probe 3 looks mostly at the voltage $\dot{V}_g$ on the gas switch hot electrode. Probe 2 looks at the voltage on the trigger electrode, $\dot{V}_t$. The monitors are 12.7-mm-diam

[a]Electronic mail: pereira@bra4a.nrl.navy.mil
[b]Also with Berkeley Scholars, Springfield, VA.

 0021-8979/96/79(1)/508/9/$6.00

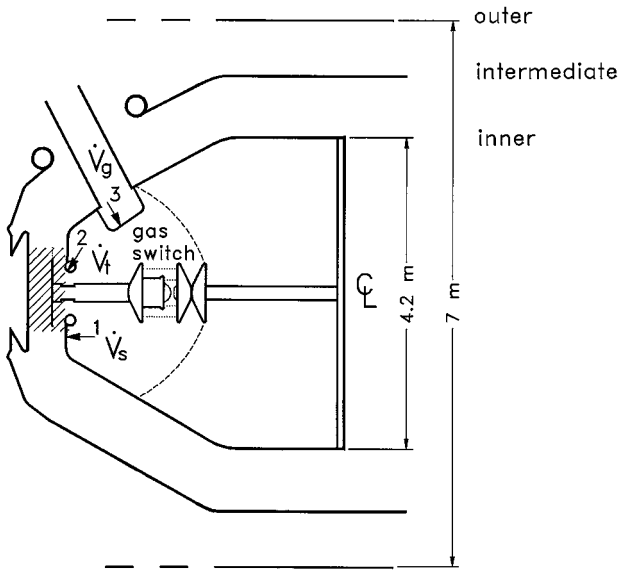

FIG. 1. Detail of the oil switch region. The numbered $\dot{V}$ monitors look at (1) the switch voltage $\dot{V}_s$, (2) the trigger voltage $\dot{V}_t$, and (3) the gas switch voltage $\dot{V}_g$. The camera's field of view is hatched.

thumbtacks stuck into a female HN connector. At 10 kV/cm ns or 10^{15} V/s m they give a healthy $\simeq$125 V signal, vastly exceeding the $\sim$10 mV noise. The calibration accuracy is only about 25%. Calibration does not affect timing and pulse shape, which are the principal quantities of interest here. However, the absolute values of voltage or current, and especially power or energy, are not as reliable as we would like.

On a sample shot, 8822, Fig. 2 surveys the time derivative of the voltage on the oil switch trigger electrode, $\dot{V}_t$. Charging takes from about -1500 to 0 ns. In this time the trigger voltage increases to about $+0.8$ MV, and the switch voltage to about 8 MV. The trigger's average voltage rate of rise $V_t \simeq 0.25$ kV/ns is too low to be seen. At trigger times, $t=0$, the gas switch fires. Now the voltage derivative on the trigger electrode starts to oscillate approximately as a

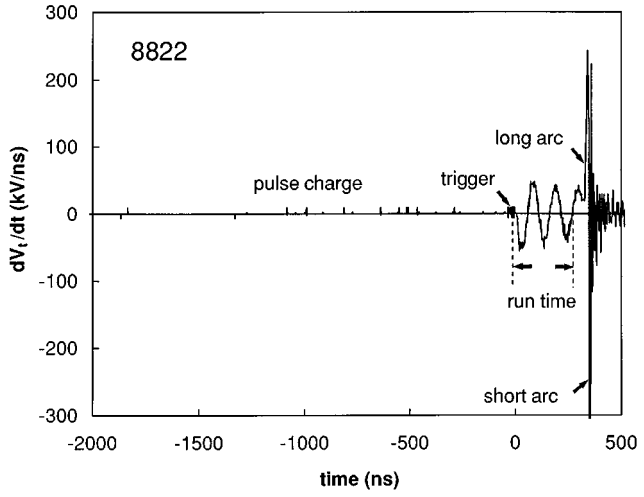

FIG. 2. Overview of $\dot{V}_t$ on the trigger electrode during charging, after triggering, and after switch closure (positive polarity shot 8822).

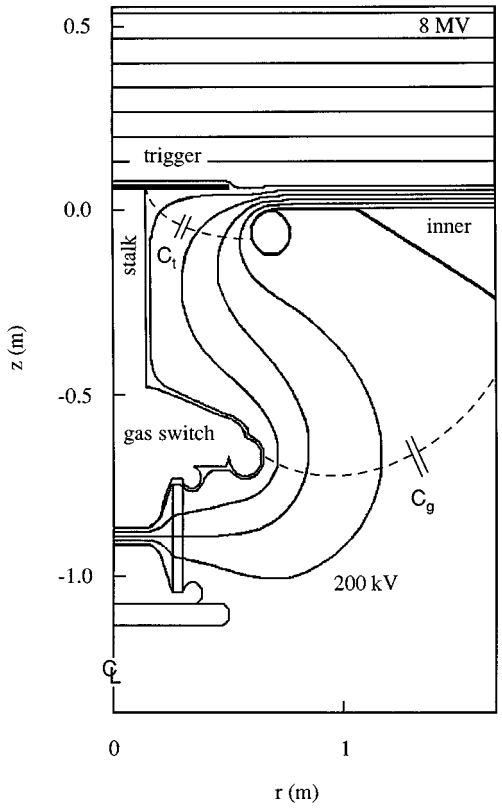

FIG. 3. Electric potential in the oil switch region after charging. Capacitance symbols suggest the regions that define a circuit element.

damped sinusoid with a 120 ns period and 60 kV/ns amplitude. The oscillation lasts until the end of the switch run time, when the trigger connects electrically through a long arc to the high-voltage electrode, at about 300 ns. The switch closes when the trigger connects to the ground electrode, about 30 ns later at the downward spike on $\dot{V}_t$. These different regimes for $\dot{V}_t$ are now discussed in detail.

A. Charging of a *V*/*n* switch

A field distortion switch is designed such that the trigger electrode remains in electrical equilibrium with the potential in the switch medium while the switch is charged. In a V/n switch the trigger voltage V_t is determined by capacitive division. That is, $V_t \simeq V_0(C_c/C_S)$, where $V_0 = V_0(t)$ is the charging voltage on the hot electrode and C_c is the capacitance between the hot electrode and the trigger. The capacitance C_S is the total stray capacitance between trigger and ground.

Figure 3 illustrates the potential in the switch region during charging. The total stray capacitance to ground C_S is given by the computation of the potential. Conceptually, C_S can be split somewhat arbitrarily into the separate capacitances as indicated, e.g., the capacitance from trigger to ground C_t, or the capacitance from the gas switch to ground C_g, and others. These individual capacitances can be estimated analytically to some degree, but the coupling capacitance between the trigger and the high-voltage electrode C_c can be determined exactly. Between the hot electrode and the trigger potential lines are flat. Therefore C_c is an ideal flat-

TABLE I. Circuit elements in two switch designs.

Element symbol	Large switch	Small switch
C_c (nF)	0.03	0.012
C_t (nF)	0.37	0.15
C_g (nF)	0.12	0.1
C_s (nF)	0.03	0.01
C_l (nF)	0.03	0.01
L_t (nF)	550	400
L_{s1} (nH)	30	30
L_{s2} (nH)	30	30
L_t (nH)	80	80
R_t (Ω)	0	20
R_l (Ω)	0	20

plate capacitor, without edge effects. From the geometry $C_c=\epsilon_r\epsilon_0\pi R^2/(l-s)$, with R the trigger electrode's radius and $l-s$ the distance to the hot electrode. Table I contains representative values.

If the potential lines at the edge of the trigger electrode are more or less flat, as in Fig. 3, the voltage on the trigger corresponds to the potential in the surrounding oil. With the high voltage electrode at l and the trigger at a stickout distance s, the voltage on the trigger is $V_t=V_0 s/l$. Figure 4 shows V_t/V_0 as function of relative stickout distance s/l. The solid line corresponds to a constant electric field in the switch, without perturbations from trigger electrode or the hole in the inner Blumlein electrode. The curved solid line is computed in the geometry of Fig. 3, for a trigger electrode with $R=0.3$ m, small enough to go through the hole in the ground electrode. In this case the trigger voltage is finite even when the trigger is flush with the ground plate, at $s/l=0$. The voltage increases with increasing stickout distance, until it is equal to the unperturbed potential at the equilibrium stickout distance s_0, where the two curves intersect.

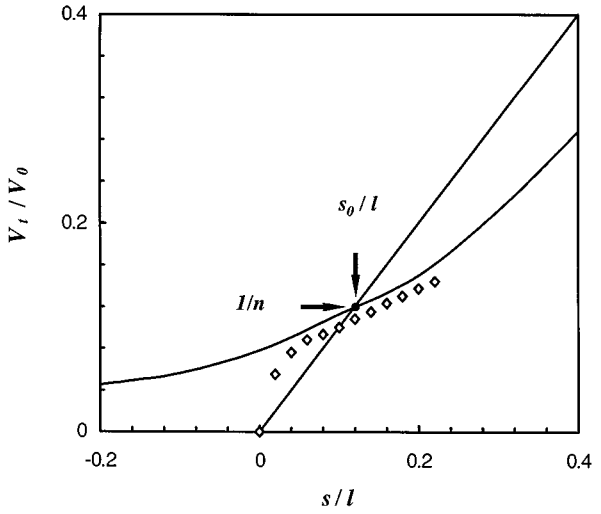

FIG. 4. Normalized voltage V_t/V_0 on the oil switch trigger electrode as function of the normalized stickout distance s/l, for a 0.5-m-diam trigger electrode. The straight line is the unperturbed potential in the oil. The open diamonds suggest the normalized voltage for the 1-m-diam trigger electrode that does not fit through the hole in the ground electrode.

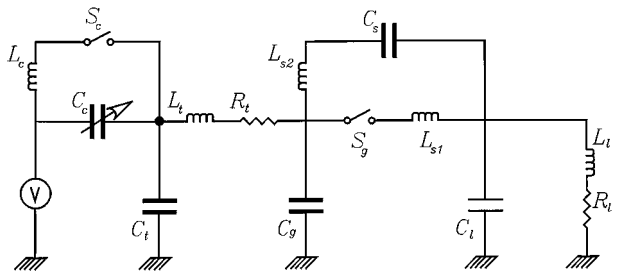

FIG. 5. Oil switch trigger circuit schematic.

Beyond s_0 the trigger voltage remains lower than the unperturbed voltage.

The open diamonds suggest the situation for a switch with a trigger electrode that has a larger radius $R=0.5$ m, too large to pass through the hole. This is the size of the electrode used in the original switch. When this trigger electrode approaches the ground electrode, $s/l\rightarrow 0$, the capacitance between trigger and ground increases as $C_g\propto l/s$. The trigger voltage decreases to zero, $V_t\propto s/l$, but faster than the equilibrium voltage.

At the equilibrium stickout distance s_0 the voltage on the trigger electrode intersects the equilibrium voltage at an angle. This angle would determine the tolerance in picking the stickout distance if it were necessary to closely approach electrostatic equilibrium. Aurora's oil switch is very forgiving in practice, tolerating stickout distances of at least $\pm 25\%$ around s_0, without spontaneous breakdowns or losing triggerability.

A high electric field at the trigger electrode's edge is often thought to be necessary for accurate triggering, and trigger electrodes are frequently sharpened in an effort to guarantee low-jitter pulses. In contrast, we show below that low-jitter triggering is possible with a dull trigger electrode, provided that a single trigger pin extends radially into the region in between switch electrodes.

Avoidance of sharp trigger electrodes is motivated by the following observations. The first shot on a freshly sharpened trigger electrode usually triggers early. Presumably, this is because an unavoidable electrostatic disequilibrium in trigger voltage is sufficient to initiate oil breakdown during the ~ 2 μs charging phase of the switch. At a dull electrode and the same voltage disequilibrium, the electric field is too small to cause spontaneous breakdown during the charging time. Then breakdown is initiated by triggering, resulting in lower jitter.

Electrostatically, the trigger voltage is uniquely determined from the capacitances, i.e., from the geometry, but how good is the electrostatic approximation? Figure 5 is an equivalent circuit for the switch region. Capacitances indicated by the thick symbols have been discussed earlier: C_c is the capacitive coupling between trigger electrode and the high voltage electrode, and the total stray capacitance to ground $C_S=C_s+C_g+C_t$. Here C_s is the capacitance between the two electrodes of the gas switch (which in Fig. 3 have 800 kV across them), C_t is the capacitance between trigger and ground, and C_g is the capacitance from the hot gas switch electrode to ground. Splitting C_t and C_g is some-

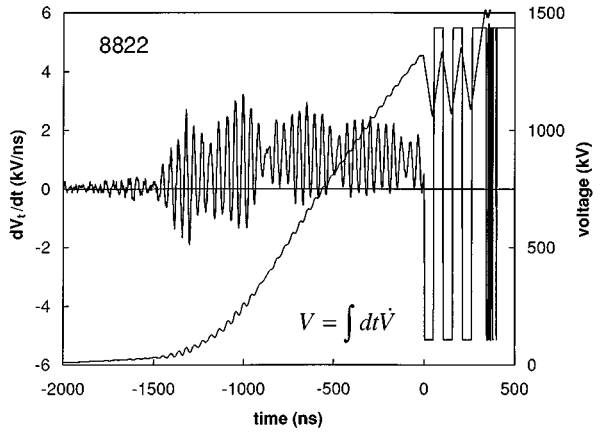

FIG. 6. Time derivative $\dot{V}_t$ on the trigger electrode, on a sensitive scale appropriate for the pulse charge (positive polarity, shot 8822). Fast oscillations stand out. The same oscillations on the voltage $V_t = \int dt\, \dot{V}_t$ (the dashed line) are difficult to measure directly.

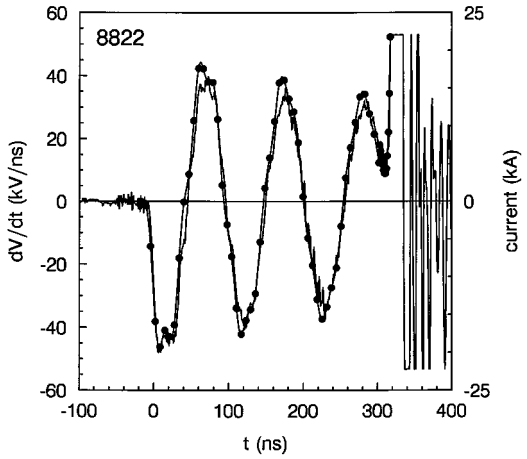

FIG. 7. Comparison between $\dot{V}_t$ on shot 8822 and $\dot{V}_t$ from the circuit.

what arbitrary, because each contains an arbitrary part of the distributed capacitance for the stalk. A reasonable boundary between the two capacitances is suggested by the dashed field line in Fig. 3. In terms of these capacitances the trigger voltage in the electrostatic approximation is $V_t = V_0/(C_S/C_c + 1) = V_0/n$. The factor $n = (C_S/C_c + 1)$ is a number $n \gg 1$ if the stray capacitance $C_S \gg C_c$.

Table I contains reasonable values for the different circuit elements, derived from a combination of computations and measurements. As an example, for the large switch $C_S \simeq 0.45$ nF while $C_c \simeq 0.03$ nF, and $n \simeq 15$. The maximum trigger voltage is then about 0.5 MV, 1/15 of the nominally ~ 8 MV peak voltage across the switch.

Electrostatically, the low-voltage electrode of the gas switch is connected to ground by its support, the T-shaped structure on the right-hand side of Fig. 1, and by the dashed lines that are in reality braid or copper sulfate resistors. In the circuit these elements are represented by the inductance L_l and the resistance R_l. Similarly, the inductance L_t represents the stalk between the trigger electrode and the hot gas switch electrode, and L_{s1} is the inductance accompanying the gas discharge in the switch. The rf cavity formed by the gas switch electrodes is mocked up by L_{s2} together with C_s. In later uses of the circuit the coupling capacitance can change with time, $C_c = C_c(t)$, to represent the electrostatic component of arc propagation, while L_c represents the inductive component. Closure of the gas switch is accounted for by the switch S_g, and closure of the oil switch by S_o, circuit components whose resistance varies nonlinearly in time.

Deviations from electrostatic charging are evident in Fig. 6, which shows $\dot{V}_t$ on a fine scale during the pulse charge. Instead of the expected pulse charge wave form, a sinusoid with $\dot{V}_t \simeq 0.25$ kV/ns between -1500 ns and triggering at $t = 0$, the signal is dominated by regular oscillations. The maximum is $\dot{V}_t \cong 3$ kV/ns, while the minimum is negative, about 1 kV/ns. The period is around 40 ns, with an additional modulation of the envelope at about 700 ns. At triggering, $t = 0$, the data go off-scale. Integrating over time gives the voltage (dashed line), whose overall shape corresponds to the sinusoidal pulse charge. On top of this are fast oscillations with $\Delta V_t \simeq 20$ kV, a few percent of the $\simeq 500$ kV trigger voltage V_t.

In principle the fast oscillations could affect switch timing. In this case a part of the jitter would be proportional to $\Delta V_t / V_t \simeq 4\%$. If the fast oscillation were the sole source of jitter, the 4% voltage uncertainty might cause more than 4% uncertainty in switch timing, equivalent to a jitter of up to 12 ns for a 300 ns switch run time. In any case, it seems prudent to suppress any unintended oscillation in the trigger circuit, or anywhere else for that matter. Shipman used resistive damping in the water switch on the Gamble II machine at NRL.[2] Likewise, replacing the conducting stalk between the trigger electrode and the gas switch with a resistor $R_t \simeq 20\ \Omega$ inside a nylon support stalk suppresses the fast oscillation.

B. Run time after triggering: Positive polarity

Once the switch is charged it is ready to be triggered. This is done by a pulse from the outside, which triggers the nominal 1 MV trigatron gas switch. As seen in Fig. 2, closing the gas switch at $t = 0$ sets up a high-amplitude oscillation on the oil switch trigger electrode, with $\dot{V}_t$ up to 500 kV/ns and a period around 100 ns. In 50 ns the trigger voltage changes from approximately electrostatic equilibrium to twice the voltage on the trigger, $2\Delta V_t \simeq 1.6$ MV. The trigger electrode geometry translates this voltage disequilibrium into a large (~ 100 MV/m) electric field that initiates breakdown in the oil. Our data are insufficient to determine a breakdown threshold.

Figure 7 compares $\dot{V}_t$ for shot 8822 (the solid line) with the voltage derivative on the trigger electrode computed at the node connecting C_t and L_t in the circuit for Fig. 5 (the solid circle). The model and measurements are very close, comparable with the differences from shot to shot. Clearly, the circuit describes the electrical behavior during the run time quite well until about 50 ns before oil closure at about 300 ns, when different shots diverge. The current to the trigger electrode is estimated directly from $I = \dot{Q} = C\dot{V}$ (the right-hand scale in Fig. 7).

Based on the excellent agreement between the circuit model and the measurements at a single node, currents and

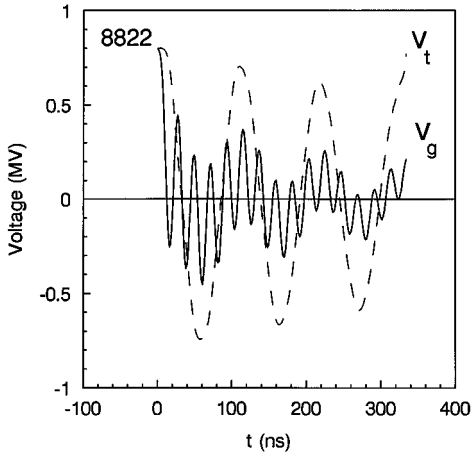

FIG. 8. Voltage $\dot{V}_t$ on the oil trigger electrode in the circuit model (the dashed line) and voltage V_g on the gas switch (the solid line). Both voltages have their own frequency.

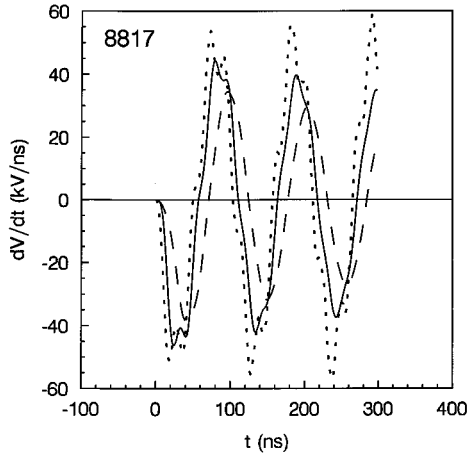

FIG. 9. $\dot{V}_t$ on the trigger electrode for different gas switch closure times. The solid line for 3 ns closure time best matches the data. An ideal switch with closing time 0.1 ns (dotted line) gives overshoots, 10 ns closing time (the dashed line) gives excessive damping.

voltages throughout the switch region can be inferred from the circuit model. The dashed line in Fig. 8 is the circuit's voltage on the trigger electrode. Despite the sharp corners and other deviations from a sinusoidal shape in the derivative $\dot{V}_t$, the trigger voltage V_t itself looks like a slightly damped sinusoid. This wave form is easily reproduced by a circuit that contains only a single capacitor C_S and a single inductor L_S. Figure 5 shows the capacitors that make up C_S in bold, while $L_S \simeq L_t + L_l$.

Simplifying the circuits of Fig. 5 to an RLC circuit omits the high-frequency components related to the various separate capacitances (C_g, C_s, and the like) that dominate the voltage V_g on the gas switch, the solid line in Fig. 8. Although these rapid oscillations should not influence oil switch timing, they are important to the gas switch. Unfortunately, the sensor facing the gas switch (No. 3 in Fig. 1) is not specific enough for rigorous comparison between measurements and computations. Only for the first 100 ns or so does the $\dot{V}_g$ as seen by the sensor agree with the circuit computations.

Closing the gas switch suddenly, changing the resistor that represents S_g in Fig. 5 from ∞ to 0 in an infinitesimal time, does not agree with the measurements. Instead, the proper closure rate and the proper final resistance must be chosen. The gas switch resistance is represented as the gas discharge member[19] of a family of switch descriptions[20] by

$$\frac{dR}{dt} = -\frac{1}{V_G^2 \tau_G} R^3 I^2 \left(1 - \frac{R_\infty}{R}\right).$$

Here V_G is a typical voltage across the switch (0.8 MV, say) and τ_G is the corresponding time scale for resistance changes. In this description the resistance decreases from its initial value R_0 at time $t=0$ to $R_0/2$ after deposition of an energy[19] $W = \int I^2 R dt = V_G^2 \tau_G / R_0$. Eventually the resistance asymptotes to R_∞, here 5Ω.

Figure 9 compares $\dot{V}_t$ computed with the circuit for an initial gas switch resistance $R_0 = 500\Omega$, and three values of τ_G. The solid line is for $\tau_G = 3$ ns, the closure time that best mimics the data (see Fig. 7). The dotted line is for an ideal gas switch that closes in 0.1 ns, while the dashed line is for a switch with $\tau_G = 10$ ns. The fast-closing switch shows spikes in $\dot{V}_t$ that are absent from most measurements. However, on rare shots $\dot{V}_t$ looks like the dotted line for a fast-closing gas switch. On these shots the gas switch might have closed faster than normal, perhaps because it was about to self-fire. As expected. the slowly closing switch gives a smoother $\dot{V}_t$ that decays faster than the measurements indicate: no shots look like this.

The energy needed for initial breakdown, $W_b = V_G^2 \tau_G / R_0$, is $W_b = 4$ J for $\tau_G = 3$ ns and 12 J for $\tau_G = 10$ ns. Most of the energy dissipated in the gas switch is deposited in R_∞ by the current through the gas switch ($\sim$10 kA average) during the $\sim$ 300 ns run time. Approximately, $W_\tau \simeq 110$ J for $\tau_G = 3$ ns and 140 J for $\tau_G = 10$ ns. The total energy deposited in the gas switch can be reduced by limiting the current with the resistor R_t. Such a resistor might lengthen the time in between gas switch maintenance.

C. Run time after triggering: Negative polarity

In negative polarity, Aurora's original bremsstrahlung mode, the oil switch circuit behaves somewhat differently from the positive polarity shots discussed up to now. Due to breakdowns elsewhere in the system, positive polarity shots use 86% lower voltage than the negative polarity shots. Therefore, positive polarity shots have a longer run time ($\simeq$300 ns) than negative polarity shots. Figure 10 is the $\dot{V}_t$ on shot 8864—negative polarity. The switch run time is about 200 ns, as expected from the ratio between the Marx charge voltages (negative 145 kV, positive 125 kV).

The open circles give $\dot{V}_t$ computed from the circuit. In negative polarity the computed V_t disagrees substantially with the measurements, which virtually overlap on nominally identical shots (except when approaching the closure time). The discrepancy might reflect additional current from activity in the oil that is specific to negative polarity.

Figure 11 is a time-integrated optical photograph of oil arcs in negative polarity. The fields of view (hatched in Fig. 1) includes the trigger electrode where the arcs are connected, and the ground torus about 5 cm away on the right-

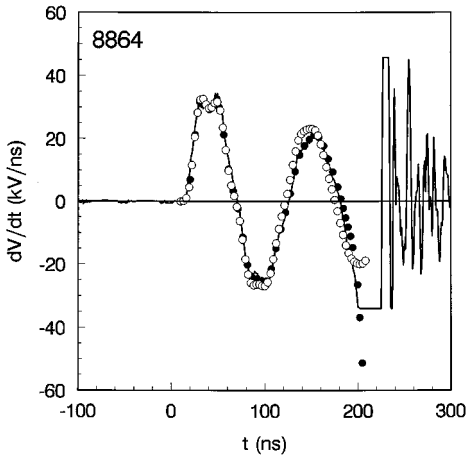

FIG. 10. Comparison between $\dot{V}_t$ on shot 8864 and $\dot{V}_t$ from a circuit model. The open dots that deviate from the measurements are for 0.03 nF trigger capacitor, the solid dots that agree include time variation in the capacitor.

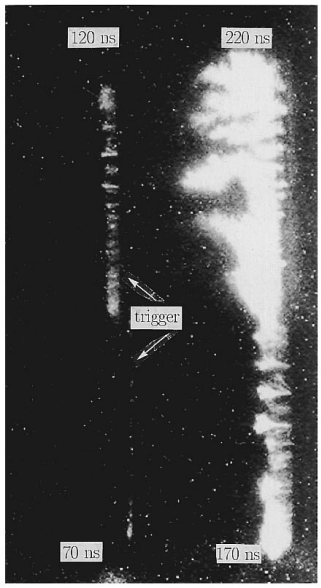

FIG. 12. Time-resolved photograph of a similar discharge. Four 10-ns-wide optical pictures of arc triggering at 70 ns, slow arc development at 120 ns, arc growth at 170 ns, and switch closure at 220 ns (negative polarity, shot 8864).

hand side. The partially light-reflecting high voltage electrode is about 50 cm away to the left-hand side. Four long arcs close the gap, while many partial arcs aspire to closure but do not seem to get there. On the short side there is a much larger number of short arcs. These come from the long side, but reverse path and end up at ground. The reason is that these arcs, with their sharp ends, are still close to ground when the long arcs hit and the voltage reverses. Positive polarity (not shown) is different: only a single arc with many branches bridges the switch gap, while at least 19 short arcs bridge the short gap. In both cases, negative and positive polarity, the switch closes fine, and the rise time of the output pulse is acceptable. Apparently, in Aurora the number of arcs is not so important.

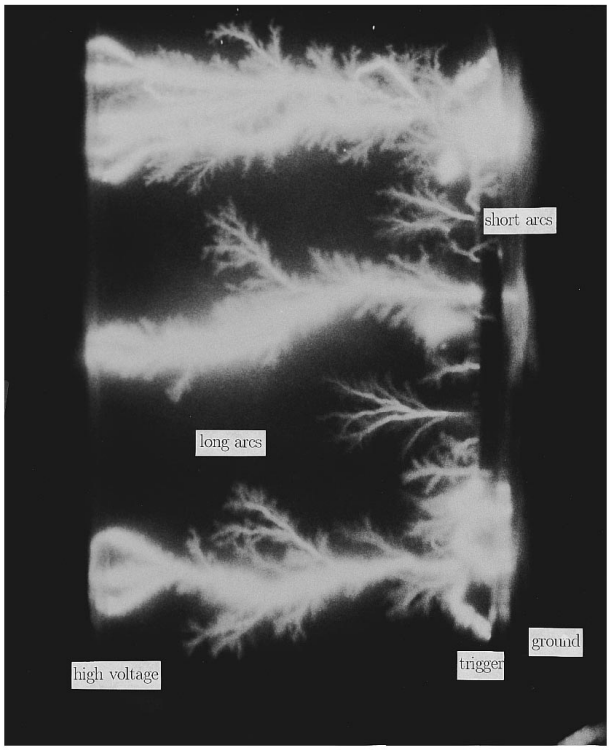

FIG. 11. Open shutter photograph of arcs for a negative polarity shot. Notice the partial arcs in the large gap, and the many closing arcs in the small gap. Closure is through only a few arcs.

Figure 12 shows four frames with 10 ns worth of arcs every 50 ns, as seen by Hadland 790 framing camera.[21] The field of view is slightly smaller than in Fig. 11. It includes the trigger electrode close to the ground electrode on the right-hand side, but barely misses the hot electrode on the far left-hand side. The pictures overlap vertially, with the one at 70 ns after triggering slightly to the right of the one at 120 ns. This is especially annoying for the pair at 170 and 220 ns.

The first frame, 70 ns after triggering, has only a sliver of light at the trigger electrode's rim, seen end-on as a 1-m-high line. At 120 ns there is light up to 5 cm into the switch gap from more than 20 arcs. The arcs are approximately the same length, but the slightly longer arcs appear to be more luminous than the shorter ones. Again, 50 ns later all arcs have grown, but the longer arcs (with about 15 cm length) have run away from their ~5 cm shorter siblings. The switch closes at 220 ns in the last picture. Only a few (here at least one, but perhaps three) arcs reach the hot electrode across the 50-cm-wide gap, while most others remain far behind at about 15 cm.

The optical length of the arcs as a function of time defines an arc propagation speed. Early on the many arcs seem to propagate at about 1.5 mm/ns. Once a few arcs stand out from the rest, as in Fig. 12 at 170 ns, the arc speed increases to about 10 mm/ns. The arc speed defined by the light emission is presumably correlated with the closure velocity of the oil switch. For the closure velocity $U_{\mathrm{av}}=l/t_r$, the literature[1,2] provides such estimates as $U_{\mathrm{av}}l^{1/4} \simeq 80V^{1.6}$. Here the voltage V is in MV, the switch gap l in cm, and the run time t_r in ns. The run time $t_r \simeq 12.5d^{5/4}/V^{1.6}$ depends strongly on voltage, decreasing from 300 to 240 ns as the Marx charge increases from 125 kV (for a positive shot) to 145 kV (for a negative

shot). It is somewhat surprising that the run times scale this well despite the polarity difference, because arcs in positive and negative polarity do not look alike.

Aurora's oil switch closing time (200 ns) is substantially longer than estimated from the literature ($\simeq$60 ns). However, the 60 ns estimate agrees with the 50–100 ns closure time of the fast arcs. Extensive measurements[9] in a planar geometry like Aurora's oil switch give for t_c a different formula that matches the data much better,

$$\left(\frac{V_0}{d}\right)^{\alpha}\int_0^{t_c} f(t)^{\alpha}dt = 21 \text{ ns}.$$

Here V_0 (in MV) is the initial voltage between the two electrodes, d (in cm) is the interelectrode distance $d=l-s$, and α is 1.3. The function $f(t)$ accounts for a possible time dependence of the voltage on time, $V=V_0 f(t)$. Here the time dependence $f(t) \simeq 1 + \delta\cos(\omega t)$ can be ignored because the voltage change on the trigger electrode, $\Delta V_t/V_0 \simeq \delta\cos(\omega t)$ is small, $\delta = 1/n \lesssim 0.1$. A change in voltage during the closure time t_c from the continuing pulse charge, $\Delta V_0 \simeq V_0(t+t_c) - V_0(t)$, can also be ignored.

Is the voltage on the trigger circuit affected by the electric activity in the oil that is related to the visible arcs? Arcs are electrically conductive, and the front of an electrically conductive region (which may or may not coincide with the visible light) should be an equipotential surface. If a conductive front moves into the oil together with the arcs, the coupling capacitance C_c should increase,[22] perhaps inversely proportional to a typical arc distance to the hot electrode. The framing photographs show a continuous light front moving halfway into the gap over the first 100–150 ns after triggering. The capacitance would increase twofold if the light front were to be an equipotential surface. Afterwards, the light front remains stationary while one or two arcs take off. Individual arcs have little capacitance, but eventually these arcs will form resistive paths. Their contribution is represented in the circuit of Fig. 5 through a variable resistance (shown as a switch) in series with an inductor, L_c.

The solid dots in Fig. 10 show what happens when the trigger electrode's capacitance $C_c(t)$ increases from 0.03 nF initially to 0.09 nF after 100 ns. The circuit now matches the data (the solid line) much better than the open circles for a constant (0.03 nF) trigger capacitance. The 0.06 nF increase in $C_c(t)$ makes the total capacitance of the trigger electrode go from about 0.4 to 0.46 nF, with a corresponding decrease in oscillation frequency of only 7%. Still, the current added to the circuit, $I(t)=\dot{Q}=\dot{C}_c V_0$, can be substantial because the changing capacitance looks at the high voltage V_0, which in a V/n switch is $n\simeq 10$ times larger than the typical voltages in the trigger circuit.

The measurements are not accurate enough to determine an effective capacitance $C_c(t)$ from the added current $I_c(t)$. Still, the threefold increase of capacitance needed to match the measurements does not contradict the twofold capacitance increase inferred from the arcs' light front: apparently some effective equipotential stretches further into the gap than the light.

When the arc reaches the hot electrode the space charge disappears from the gap, and the gap's electrical representation should no longer be a capacitor but a (time-varying) resistor in series with an inductor. This inductor, L_c in Fig. 5, is about 350 nH. The average 7 nH/cm inductance over the 50-cm-long gap corresponds to a single conducting channel with a radius r_c and a return current radius r_r such that $\ln(r_r/r_c) \simeq 3.5$. These estimates seem compatible with the optical pictures, but they are not precise enough to be analyzed much further.

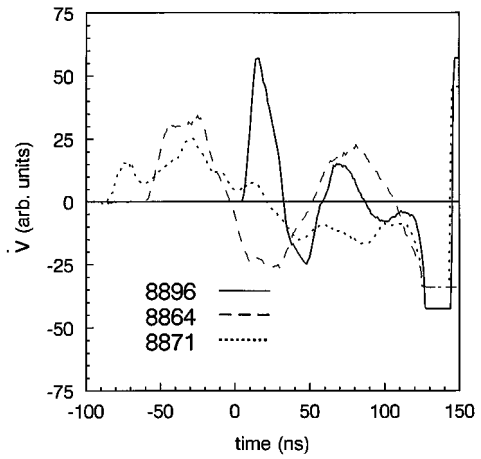

FIG. 13. Comparison between $\dot{V}_t$ in the three different switch geometries: the high-inductance original switch (the dotted line), the standard switch (the dashed line), and the resistively loaded switch with a small trigger electrode.

III. TOWARD MORE ACCURATE TRIGGERING

As is well known, triggering becomes more precise by increasing the voltage rate of rise on the trigger. This can be implemented by reducing capacitances and inductances in the trigger circuit to their lowest practical values, and by introducing a resistor that damps the trigger circuit. A resistor has been implemented in a water switch on Gamble II at NRL designed by Shipman[2] (however, in Gamble II's present oil switch[23] the resistor is replaced by an inductor). As discussed earlier, it might also help to suppress any fast oscillations during the pulse charge. These measures have to do with the electrical parameters of the trigger circuit.

Simple changes to the basic switch geometry of Fig. 1 increase $\dot{V}_t$ more than twofold. Figure 13 compares $\dot{V}_t$ for the original[6,3] oil switch trigger geometry (dotted line) with $\dot{V}_t$ for the modified version of the switch (dashed line) that is now Aurora's standard. The solid line is $\dot{V}_t$ for a switch with the smaller trigger electrode and a single trigger pin and will be discussed below.

In the original configuration the trigger electrode is connected with a ~2-m-long axial cylinder to the high voltage electrode of the gas switch. The low voltage electrode is connected by a similar pipe to a ~4-m-long support structure: additional mechanical support is provided by isolating straps that are not shown in Fig. 1. The return current structure represents about 2000 nH inductance, L_l in Fig. 5. This large inductance results in a ~200 ns oscillation time for the trigger voltage, long enough to keep the trigger electrode under charge during the switch run time. This was thought to

be needed to keep the arcs propagating. Aurora's standard oil switch bypasses the 2000 nH inductor with shorting straps. These are dashed lines in Fig. 1, and the corresponding $\dot{V}_t$ is a dashed line in Fig. 13. Despite the voltage reversal on the trigger during the run time, the standard switch gives at least comparable jitter to the original switch, approximately 8–20 ns (depending on maintenance, etc.). A clear advantage of the standard switch is that high electric fields inside the inner Blumlein are restricted to a much smaller volume, leaving room for other hardware such as mechanical supports for the Blumlein structure.

The highest $\dot{V}_t$ to date, the solid line in Fig. 13, is achieved by shrinking the size of the entire switch, within the limits of the existing parts. The trigger electrode's diameter is halved from 1 to about 0.5 m, so that the total capacitance of the trigger electrode is reduced from 0.44 to 0.17 nF (including the stray capacitance). In addition, the metal stalk that supports the oil trigger electrode is replaced by a damping resistor $R_t \simeq 19\Omega$, later increased to 30Ω. The resistor's inductance L_t is minimized by reducing its length from about 1 to 0.6 m. Through all these measures the peak $\dot{V}_t$ increases 2.5 times. Moreover, the resistance suppresses the oscillations during switch charging.

When the jitter is a constant fraction of the switch run time, the jitter decreases as the run time becomes smaller. On Proto I at Sandia National Laboratory the jitter is about 4% of the run time.[24] Increasing $\dot{V}_t$ and reducing the run time were the principal thrusts in Aurora's first jitter suppression efforts.[9]

Once the arcs are initiated, a further factor in the jitter is the reproducibility of the arcs themselves. In the standard switch the trigger electrode is a 1 meter-diam disk with a sharp edge, which gives rise to a two-dimensional arc pattern, see Fig. 12 at 120 ns. In two dimensions any arc has two close neighbors, whose electric potential makes the field on a small arc smaller, but keeps the field large on an arc that sticks out. Therefore, the longest arc should grow faster than the others: an array of arcs in two dimensions is unstable. In any unstable situation low jitter is difficult to achieve. One attempt at reducing any jitter from interfering arcs is to use a single arc, or possibly multiple parallel arcs that are far away from each other.

In pulse power machines with a low inductance Z (e.g., $Z \lesssim 1\Omega$) a single arc is not allowed, because its inductance L is usually too high for an acceptable rise time $\tau \simeq L/Z$. However, on Aurora with $Z \simeq 20\Omega$ there is no problem. Moreover, putting the single arc in the Blumlein's symmetry plane gives a highly reproducible output pulse.

With the small trigger electrode a single arc is initiated with a 10–15-cm-long pin that sticks out sideways in the trigger electrode's plane. In order to avoid unintentional arcs the trigger electrode is now rounded. An additional benefit is that a single arc propagates faster than multiple parallel arcs, giving a shorter switch run time.

The run time for small switch that initiates a single arc is about 120 ns. The original and standard switches (dotted and dashed lines in Fig. 13) have much longer run times, about 225 and 200 ns. These run times agree with measurements on multiple-arc switches with Proto I and Aurora.[25] From

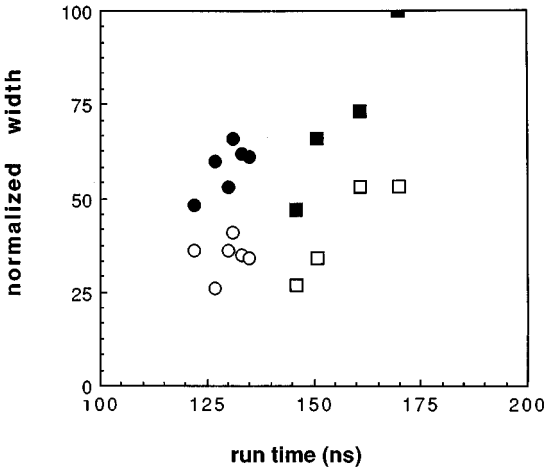

FIG. 14. The width of a single arc plotted against switch run time. The circles are for an average electric field in the switch about 10% higher than for the squares.

these measurements the run time as function of peak voltage V (in MV) matches a simple scaling relation, $t_c = l/u$ with the average closure speed $u = 0.37\ V$ with u in mm/ns. For a peak pulse charge voltage $V \simeq 8$ MV the average arc speed is 3 mm/ns, and the run time over the 55 cm gap would be about 185 ns. For the standard switch the run time is indeed $t_c \simeq 185$ ns, 25×longer than the jitter, with $\sigma \simeq 8$ ns. However, the switch with the single point trigger is substantially faster, down to $t_c \simeq 125$ ns.

A shorter run time with a single arc is reasonably consistent with its ≃8 mm/ns apparent propagation speed, much faster than the ≃2 mm/ns speed of multiple parallel arcs that occur early on in the switches with sharp trigger electrodes. If an arc were to propagate at a constant 8 mm/ns speed starting at the trigger time, the closure time would be still lower, perhaps 60 ns. The ratio between the 125 ns run time and the 4 ns jitter remains about 25.

Switch run time appears to be correlated with the transverse size of the arc as it appears on the framing photographs. Figure 14 shows the width of the single arc plotted against run time. The definition of arc width is somewhat arbitrary, because it is hard to decide what separates arc light from dark oil: the width was measured from the scanned picture by an unbiased observer. The arc width appears to be well correlated with run time for the squares. These shots have a large (10 ns) spread, and an electric field in the switch gap that was on the low side, about 10% less than for the shots corresponding to the circles. Even for these much tighter arcs, with smaller widths, there is a hint of a correlation. Five of these shots fall within an 8 ns window, for a 1σ jitter of less than 3 ns. Including all six shots gives a 13 ns window, and 1σ jitter of 5 ns. Unfortunately, the single day of shooting available for these measurements is not enough to determine the jitter more precisely.

That the apparent arc width and the run time might be connected is more or less understandable. Sometimes a wide arc originates in two parallel arcs propagating from the same initiation point. As is the case with the many arcs in the two-dimensional switch, two parallel arcs have an electric

field at the arc tips that is lower than for a single arc. The resulting slower arc propagation speed could cause a later closure. Other times a single arc appears to wander around in the switch gap, presumably taking longer to cross, even though it might have the same linear speed (or the same field at its tip) as an arc that goes straight.

Once there is a single arc it might be possible to reduce jitter further by letting this arc follow a preselected path in the oil, analogous to the straight lightning strokes that follow a wire trailing a rocket or a laser-initiated conducting path. A preferred discharge path in the oil could conceivably be created by drifting in a string of bubbles, a line of space charge, or a column of heated oil. We have not had the opportunity to implement any of these suggestions.

That various modifications to Aurora's V/n oil switch could be tested without any problem demonstrates that the switch is remarkably insensitive to deviations from the intended operational mode. The trigger electrode need not to be in exact electrostatic equilibrium, the trigger voltage need not be synchronized with arc closure, and the number of arcs can vary from one to many. Therefore we do not expect obstacles in testing further changes, such as a designated breakdown channel to straighten out the arc.

IV. CONCLUSION

A redesigned oil switch that starts a single arc in a designated position is able to switch a nominal 10 MV Blumlein with minimum jitter, putting most shots within an 8 ns window. The switch design criteria appear to be valid, and should be useful elsewhere. These include resistive suppression of fast oscillations that could cause unintended timing variations, increasing the trigger voltage rate of rise by reducing capacitances and inductances, and making the switch run time smaller.

In a high-impedance machine, closure with a single arc improves the output pulse substantially, especially when the machine's symmetry is used to advantage. Further downstream in Aurora's pulse forming network is a prepulse switch, which has 12 self-breaking arcs in a circle. Firing only two of these gives the most reproducible pulses, provided the single arc in the oil switch is placed in the symmetry plane defined by the two prepulse arcs. This aspect of the work is presented elsewhere.[11]

ACKNOWLEDGMENTS

It is a pleasure to thank Dr. G. Merkel (ARL) for triggering this work, and Dr. J. Agee (HDL) for the initial support. Early contributions by Dr. K. Stricklett (NIST) and D. M. Weidenheimer (BRA) are gratefully acknowledged. Special thanks go to D. C. Judy for his help in data acquisition, and to A. R. Poirier and his Operations and Maintenance crew for their tremendous cooperation. The initial research was supported by DNA and the Army's Productivity Improvement Funds, with final support from BRA's IR&D.

[1] J. C. Martin, Proc. IEE **80**, 934 (1992).
[2] I. Vitrovitsky, *High Power Switching* (Van Nostrand, New York, 1987).
[3] B. Bernstein and I. B. Smith, IEEE Trans. Nucl. Sci. **NS-20**, 294 (1973).
[4] See, for example, R. B. Miller, *Intense Charged Particle Beams* (Plenum, New York, 1982), Chap. 1.
[5] See, for example, P. E. Peterkin and P. F. Williams, J. Appl. Phys. **66**, 4163 (1989).
[6] D. M. Weidenheimer, N. R. Pereira, D. C. Judy, and K. L. Stricklett, Proceedings of the Beams '92 Conference, Washington, DC (unpublished) (1992), p. 640.
[7] K. L. Stricklett, D. M. Weidenheimer, N. R. Pereira, and D. C. Judy, *IEEE Conference on Electric Insulation Dielectric Phenomena*, Victoria, B.C., 1992 (IEEE, New York, 1992).
[8] N. R. Pereira, *IEEE Pulse Power Conference*, Albuquerque, NM, 1995 (IEEE, New York, 1995).
[9] F. T. Warren, H. G. Hammon, B. N. Turman, and K. R. Prestwich, *Proceedings of the IEEE Pulse Power Conference*, Arlington, VA, 1987 (IEEE, New York, 1987).
[10] R. A. Meger, F. C. Young, A. T. Drobot, G. Cooperstein, D. Mosher, S. E. Graybill, G. A. Huttlin, K. G. Kerris, and A. G. Stewart, J. Appl. Phys. **52**, 6084 (1981); R. A. Meger and F. C. Young, *ibid.* **53**, 8543 (1982).
[11] N. R. Pereira and N. A. Gondarenko, to be presented at the 1995 Pulse Power Conference, Albuquerque, NM (unpublished); Also internal ARL publication (in progress).
[12] R. E. Tobazeon, in *The Liquid State and Its Electrical Properties*, NATO ASI Series B, Vol. 193, edited by E. E. Kunhardt, L. G. Cristoforou and L. H. Luessen (Plenum, New York, 1988).
[13] J. Fuhr, W. F. Schmidt, and S. Sato, J. Appl. Phys. **59**, 3694 (1986).
[14] A. Beroual, J. Appl. Phys. **73**, 4528 (1993).
[15] H. M. Jones and E. E. Kunhardt, J. Appl. Phys. **77**, 795 (1995).
[16] Eric O. Forster, J. Phys. D Appl. Phys. **23**, 1506 (1990).
[17] W. G. Chadband, J. Phys. D Appl. Phys. **24**, 56 (1991).
[18] See, for example, J. Sazama and V. Kenyon, *IEEE Pulse Power Conference*, Albuquerque, NM, 1979 (IEEE, New York, 1979), p. 187, and many other papers in this and subsequent conferences.
[19] R. Rompe and W. Weitzel, *Theory of Electric Arcs and Sparks* (Barth, Leipzig, 1949).
[20] N. A. Gondarenko, T. A. Golub, and A. M. Iskoldsky, IEEE Trans. Plasma Sci. **20**, 967 (1992).
[21] We would like to thank Dr. A. Fisher for his help with this instrument.
[22] G. M. Wilkinson, *Proceedings of the Fourth IEEE Pulse Power Conference*, Albuquerque, NM, 1983 (IEEE, New York, 1983), p. 323.
[23] J. D. Shipman, *IEEE Pulse Power Conference*, Albuquerque, NM, 1981 (IEEE, New York, 1981), p. 475.
[24] K. R. Prestwich, P. A. Miller, D. H. McDaniel, J. W. Poukey, M. M. Widner, S. A. Goldstein, International Topical Conference on Electron Beam Research (unpublished), Vol. I, p. 423; K. R. Prestwich, in *Energy Storage Compression and Switching*, edited by W. H. Bostick, V. Nardi, and O. F. S. Zucker (Plenum, New York, 1976).
[25] B. N. Turman, D. R. Humphreys, J. F. Seamen, K. R. Prestwich, R. A. Hamil, T. H. Martin, F. T. Warren, and G. Frazier, Sandia Report SAND86-0061 (1986).